A Review on Fabrication and Printing of Metal-Polymer Composite Filaments

[1]A.Lakshumu Naidu, [2]Ragolu Daniprasheel, [2]Panchadarla Mani Murali, [3]V. Somasekhar, [4]Palavalasa Saivikram, [5]S.D.V.M. Srinivas Reddy, [*6]V. Jayakumar
[1,2,3,4,5,6]GMR Institute of Technology, Rajam, Andhra Pradesh. 532127.

ABSTRACT
This article outlines the key concepts of filament preparation and printing of metal-filled polymer composites through FDM technology. Fused Deposition Modelling (FDM) or Fused Filament Fabrication (FFF) uses the idea of melting the material and depositing it layer by layer. The filament for this process is usually prepared by mixing the metal powder in a polymer. The extrusion method is usually the preferred way to fabricate the filament, however, the procedure for mixing polymer and metal depends on the polymer. In this article, the main processes behind various combinations; of PLA, ABS, and PVB as polymers and Aluminium, Copper, Iron, Steel, Nickel, and Ceramics as fillers have been discussed. It is concluded that this technology can have a wide range of applications from aerospace, energy storage, medicine, education, etc… Possible future prospects for further research have also been highlighted.
Keywords: Metal Fused Filament Fabrication, Metal-Polymer Composites, Additive Manufacturing, Debinding, Sintering

1. INTRODUCTION
Additive manufacturing is a process of creating three-dimensional objects by adding successive layers of material. This is the opposite of subtractive manufacturing, which involves removing material from a solid block or sheet to create the desired shape. The process of additive manufacturing typically involves three steps: designing the object using Computer-Aided Design (CAD) software, preparing the design file for printing using software that generates instructions for the printer, and printing the object layer by layer using a 3D printer. Additive manufacturing can be used to create a wide range of objects, from small, intricate parts to large, complex structures. It is used in many industries, including aerospace, automotive, healthcare, and consumer products. There are primarily seven processes recognized by International Organization for Standardization (ISO) which are; Binder jetting, Directed energy deposition, Material extrusion, Materials jetting, Powder bed fusion, Sheet lamination, and Vat Photopolymerization [1,2]
The materials which can be printed through these processes are Metals, Polymers, Ceramics, Composites, Smart materials, and Special materials [2]. Few materials can be printed through multiple processes but the metals are strictly limited to energy-intensive processes such as Powder Bed Fusion (PBF), Selective Laser Sintering (SLS), Selective Laser Melting (SLM), etc… This need for more energy makes the metal 3D printing more expensive process. The material extrusion processes such as Fused Deposition Modelling (FDM), and Fused Filament Fabrication (FFF) are the most economical. However, the feedstock for these processes is strictly limited to thermoplastics such as PLA, ABS, PVB, PC, PET, Nylon, etc…[3]
Several attempts have been made to develop new techniques to print metal through these processes. One such method is to mix metal powders of a particular size and shape in a thermoplastic filament. The process to accomplish this has been discussed in detail in the work [4]. Few studies tried to mix

carbon-based nanomaterials, ceramic powders, metal powders, glassy fillers, minerals, wood, etc... into the feedstock [5].

Confining the discussion to metals, studies have been done on several metals and alloys such as; Ti-6Al-4V, 316-L Steel, 17-4 PH Steel, Aluminium, Copper, Nickel etc…

In the works [6,7,8] Ti-6Al-4V has been taken as the main filler and studied its printability and the effects of process parameters in its printing. Few works have been reported on 316-L Stainless Steel [9,10,17] and 17-4 PH Steel [11,17]. Characterization of the mechanical properties of the objects printed through this process is equally important as well. A similar attempt has been done on wood, ceramic, metal, and carbon fibre based-based PLA composites [14]. This technique when combined with metals and ceramics will especially give an advantage to the aerospace and automotive industry [15,17]. A trail has been done to print Nickel based composite for the catalytic purposes. Ni-PVB, Ni-ABS, and Ni-PLA combinations were tried in the work [18]. Very few works have been reported on Copper [21] and Aluminium [22].

The metal based composite filaments which are obtained through this process can be printed by the printers which are intended for thermoplastics. Since, the obtained part will consist of both thermoplastic and metal, the part can be used in the same combined form or can be post-processed to obtain pure metal part. The post processing steps such as; Debinding and Sintering may alter some of the mechanical properties [24,25]. This could be an advantage or disadvantage depending on the application.

2. MATERIALS

2.1 Metals:

Due to the benefits offered by this approach, metal 3D printing technology has attracted a lot of attention in the manufacturing, aerospace, and automotive industries. Metals are good physical materials that can be employed in multiple manufacturing processes, including the printing of bones, space shuttle parts, jewelry etc… For suppose, Cobalt-based alloys are best suited for printing dental parts. Aluminum alloys are widely used in aerospace applications due to their lightweight. Titanium alloys such as Ti-6Al-4V are used in rockets and bone implants. These metals or alloys, when combined with 3D Printing technology, can aid in overcoming several limitations. [2]

Moreover, 3D printing technology may create aircraft components employing nickel-base alloys. Nickel base alloy-based 3D-printed objects can be used in hazardous locations. This is due to its strong corrosion resistance and ability to withstand temperatures of up to 1200 °C. Finally, titanium alloys can also be used to build the thing utilizing 3D printing technology. Unique qualities of titanium alloys include ductility, strong resistance to corrosion and oxidation, and low density. It is utilized in high-stress, high-temperature working environments, and high-stress applications, such as in aerospace components and the biomedical industry. [2]

2.2 Polymer:

3D Printing with polymers is used in printing complex geometries from prototypes to functional parts as well. Extruded thermoplastic filament, such as polylactic acid, can be deposited in successive layers using fused deposition modelling (FDM), which can create 3D printed objects. polypropylene (PP), acrylonitrile butadiene styrene (ABS), or polyethylene (PE). Thermoplastic filaments with higher melting temperatures, such PEEK and PMMA, are now being employed as 3D printing materials. Due to their low cost, low weight, and processing flexibility, 3D printing polymer materials in liquid state or with low melting point are widely used in the industry. In biomaterials and medical device products, polymers are typically used as inert materials and have a significant impact. [2]

2.3 Metal-Polymer:

Mixing metal powder in polymer and extruding them together as a filament is the most commonly used method for printing metal using FDM.

The composite filament is a combination of metal powder and binder system. Usually, a binder system is a thermoplastic polymer combined with some other additives or surfactants. The shape and size of metal powder particles will play a key role in defining the mechanical properties of the final product. The binder will have an impact during all four stages of MFFF [4].

Attempts are being done to print alloys of titanium, tungsten, chromium, silicon compounds, zirconium compounds etc… Some of the most popular composites are 316L Stainless Steel, 17-4 Stainless Steel, WC-10 CO, Ti(C,N), (Ta, Nb) C, Cr3C2, ZrO2, Ti – 6Al – 4 V. Along with them, a few other alloys are also being tested [4].

At least 20% of the filament should be made of powder. Unfortunately, this amount of powder will make the filament less stiff and robust, and while printing, there will be a significant material consumption when taking additional shrinkage into account. excessive amount of powder will make production more difficult. The filament will break during winding because of its high stiffness and low ductility. Moreover, a lot of metal powder will make the filament viscous. The feed mechanism will need to be strengthened, or feeding can be done manually. Mixtures with a 50–79% powder concentration are provided in works. [4]

The ideal powder concentration is between 50 and 65%. The form and size of the powder's particles are crucial factors. Generally speaking, powder metallurgy and additive manufacturing use high sphericity powders. This is essential for a uniform filament structure, which in turn impacts the filament's mechanical characteristics. Mechanical qualities are also influenced by particle size. Excessive particle size will compromise the filament's rigidity and strength, making printing difficult. Powders with particle diameters ranging from 5 to 15 mm are used in powder metallurgy. According to research, a lower nozzle size is appropriate for a smaller particle diameter. If it doesn't interfere with the printing process, powders with both smaller and bigger particle sizes can be utilised for printing. You can use powder made for powder metallurgy to produce filament. The shape and size of this powder must, however, adhere to strict standards. You can use powder made for powder metallurgy to produce filament. The shape and size of this powder must, however, adhere to strict standards.

When creating the future filament's composition, the binder system also needs to receive enough consideration. It is necessary for both the final product's quality and the accuracy of the preserved shape in intermediate stages.

Each binder system has three basic parts: the main body, the backbone, and numerous additives. 50 to 90% of the total volume is the primary component. Its function is to maintain the product's shape right away after printing and to enhance the filaments' printing-related qualities. In the initial phase of binder removal, the major component is removed. The volume that the backbone component takes up ranges from 0 to 50%. During the initial step of the removal of the binder system and the interim, the powder particles are retained. In the second stage of elimination, the component is recovered. During the product's final firing, residues are taken out. To enhance the filament's characteristics, additives are required. They take up between 0 and 10% of the total volume. These help in reducing the viscosity of the filament and also prevent agglomeration during mixing. The primary component is made out of several polymers. Many works present a variety of alternatives, but it is possible to identify a few key ones among them. These are several kinds of thermoplastics, elastomers, and waxes. Several types of primary component are provided in [8]. Systems based on wax, polyethylene glycol, and thermoplastic elastomer (TPE) have been employed in a number of investigations (PEG). Other polymers are also employed for the backbone component (poly amide, polypropylene, polyoethene, etc.). The final filament's viscosity decreases with increasing backbone component content. Assorted additions include stearic acid, plasticizers, tackifiers, and others. To avoid agglomeration, stearic acid is typically added in the powder mixing step. The qualities of the filament can be considerably enhanced by additives, for instance by lowering viscosity. Unfortunately, some

additions weaken the filament's strength. In some works, the precise make-up of the filament or the binder technique is not stated. In order to accurately decide what should be included in the composition for each unique scenario, empirical research is required. The typical scheme of Fused Filament Fabrication (FFF) is shown in fig. 1. In addition, one should think about how the composition chosen would impact subsequent technical procedures. [4]

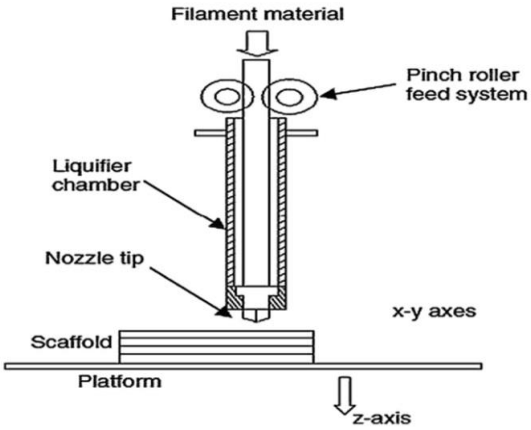

Fig. 1. The scheme of FFF [4].

3. FILAMENT PREPARATION

Successful product manufacture involves more than just choosing the future filament's composition correctly. To completely rule out the risk of product deformation during printing due to inadequate filament quality, the components must be mixed properly. Both small batches and continuous mixing can be done. Several grinders and mixers can be utilized in the first scenario. Screw extruders work well in the second scenario. To improve homogeneity, the powder must first be put through a filter. Certain powders must also be treated with stearic acid to stop agglomeration. The next step is to combine the metal powder with the binder system before feeding it into the extruder. In several texts, the filament production process is explained in a variety of ways. But the major goal is to provide the finished filament the proper amount of toughness, roundness, strength, and stiffness. Low strength and stiffness will cause the filament to break, whereas high viscosity, stiffness, and inadequate roundness will make it difficult to feed the filament. As a result, it's crucial to choose the proper extruder operating modes, production temperature settings, and shape control procedures while creating filament. The finalized filament is wound onto spools in the last step, which are then put right into a 3D printer to produce the object. [4]

3.1. Ti-6Al-4V:

The Ti-6Al-4V-based composite filaments are made in a similar process as discussed above. Metal-Fused Filament Fabrication (MFFF) is a method for producing metals additively that relies on highly filled metal powder-polymer filaments. The thermoplastic polymer acts as a binder which consists of metal particles mixed in it. This binder also helps in the flow of the material during material extrusion-based printing. The schematic of MF3 process for Ti-6Al-4V is shown in fig.2. The printed parts will then be followed by the post-processing steps such as debinding and sintering at higher temperatures which will densify the final parts [6].

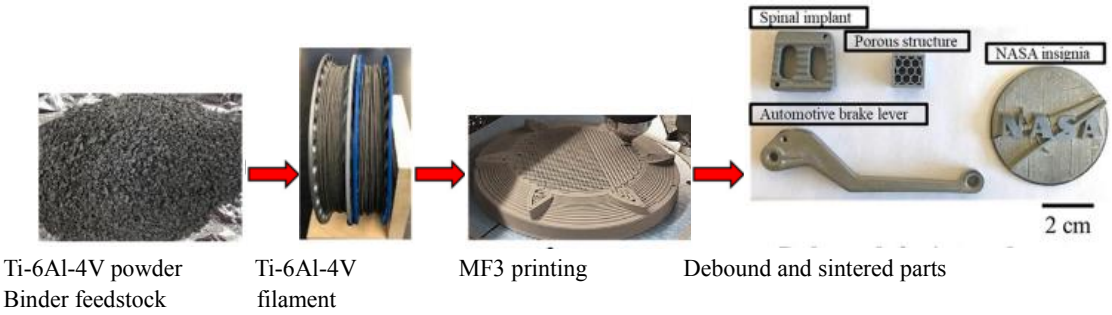

Fig. 2. Schematic of MF3 process for Ti-6Al-4V. [6]

The metal-polymer-based raw material which is used to make filaments need to have a viscosity that is low enough to allow for smooth extrusion of material at particular extrusion speed and printing temperature. The feedstock viscosity is affected by shape and size of the powder particles. Due to their outstanding flow and filling properties, spherical particles 45 m are typically selected to produce denser filaments and low viscosity. Also, the size of the powder particles that can be used depends on nozzle diameter and the material of the nozzle. The flow of the filament increases with an increase in feed rate. This results in an increase of pressure drop at the exit of nozzle and necessitates a greater effort to keep the material flowing continuously. Because, failures in print may occur due to shear during higher feedrates [6].

The powder particles in the work [6] has been classified as fine and coarse. 13µm size is considered as fine particles and 30µm is considered to be coarser. These powders are taken in 59 vol% (87 wt%) and mixed with a thermoplastic binder. The mixing of raw material was done at 180□ and at 100 rpm for the blade (Brabender CWB, IntelliTorque Plasti-Corder). It is found that 64vol% is the critical loading point for fine powder mixture and 63 vol% for the coarse powder feedstock with the aid of a torque rheometer. However, for smoother filament extrusion, 59 vol% of Ti-6Al-4V powder has been taken for both fine and coarse powder. The Knurled wheel mechanism of filament is shown in fig.3. This mixture is then extruded into filaments with a 1.75±0.05mm diameter. Extrusion was done at a temperature of 105□ and at 0.1mm/s extrusion speed [6].

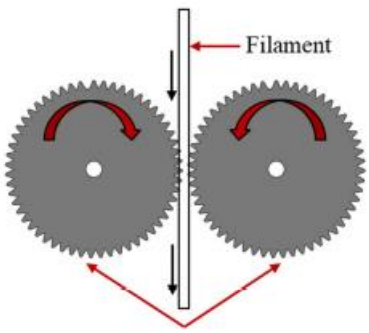

Fig. 3 Knurled wheel mechanism [6]

3.2 316L Stainless Steel:

A commercial printer that is readily available in the market is used for printing. The printer can print parts upto 200mm in all three dimensions, however the vacuum tube furnace prevented larger parts from being used in this investigation (approx. 20 mm diameter). The nozzle is made up of hardened steel and of diameter 0.6mm. Simplify3D is used as the slicer software. Simple geometric forms but with features that are limitations for MIM components are taken as test parts. Thick walls, and thickness changes are few such limitations. All bodies were printed with 100% infill density and with a 45-degree internal infill angle offset per layer. Two wall layers are given during slicing. The layer

height for each layer while printing was 0.2 mm. Only the first layer is printed with a 105% extrusion multiplier. This results in a high green body density [9].

The multicomponent binder system was eliminated using a two-stage debinding procedure that included solvent and thermal debinding phases. The printed parts are submerged in cyclohexane for predetermined durations of time in a laboratory setting to perform solvent debinding. Since, no distillation circle is built for recuperation of the solvent, it is constantly refreshed to avoid saturation. The weight loss following various debinding times was used to gauge the amount of removed polymer. After drying, the sample was weighed to determine the weight loss percentage of the polymer. The amount of polymer to be removed by weight is determined relative to the total amount of thermoplastic elastomer in the part because only the principal binder is removed. Debinding is considered complete when 99% of the polymer is extracted. The pieces were heated in a vacuum furnace during the thermal debinding process. Pressures ranged from 10-3 to 10-5 mbar considering the amount of evaporated binder that was present in the furnace at different times during the burnout process. According to the backbone polymer's thermogravimetric study, debinding temperatures were assessed. The goal of the heating process was to heat the samples as quickly as possible without causing any scorching or cracking. [9]

To avoid the steel particles oxidising at high temperatures, the fully debound components were sintering in a vacuum environment at a pressure of 103 mbar. In this investigation, no reducing gases like H2 were employed. To maximise sample densification, sintering temperatures and timings were adjusted. The Archimedes' method with water immersion technique was used to estimate the sintered density (SAG 204, Mettler Toledo, USA). SEM and energy dispersive x-ray spectroscopy (EDX) (Zeiss Crossbeam 540, Germany) were used to analyse the microstructure and element concentration. The Cross-section of the 316L particles embedded filament and powder particle size distribution is shown in fig.4. Three-point bending tests were used to assess the samples' mechanical characteristics [9].

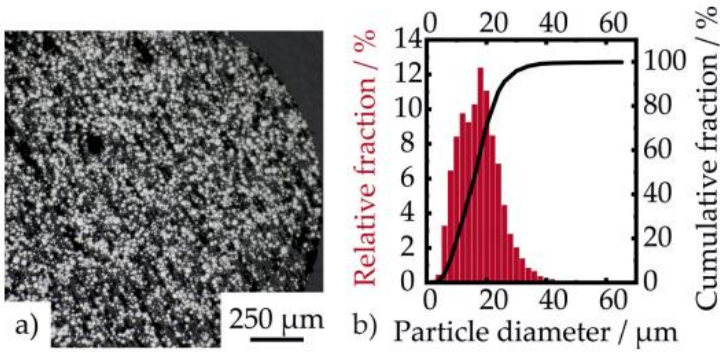

Fig. 4. (a) Cross-section of the 316L particles embedded filament (b) powder particle size distribution [9]

3.3 PLA and 316L:

316L Stainless Steel powder and PLA pellets are combined in a ball mill for three hours at room temperature. The powder particles are of size between 20µm-50µm. Samples are separated into four groups with a volume percentage of 0%, 5%, 10%, and 15%. A single-screw extruder is used to create filaments after the powder and pellets are mixed. The screw speed is 30RPM and the extrusion temperature is 105□. Forced convection is created using a fan airpath to cool the filament. This resulted in a filament of uniform diameter 2.85±0.15mm. The FFF process is carried out on a desktop 3d printer which is intended for thermoplastics. Fig 5b shows a three-dimensional porous scaffold that is manufactured for the project along with a 3D printer [10].

In particular, a row of eight parallel struts with a height of four layers are the first thing for the extrusion nozzle deposition. Each strut has a 0.8 mm width and height. The printing orientation is then

turned 90 degrees and eight more struts were layered after that. The detailed view of Lulzbot TAZ 6 3D printer and 3D structure of PLA-based scaffolds is shown in fig.5. A total of 60 layers are deposited to build a cube with 12mm side and an interconnected pore with a dimension of 0.8 mm. The FFF process parameters for fabrication of PLA-based scaffolds is shown in Table. 1 [10]

.

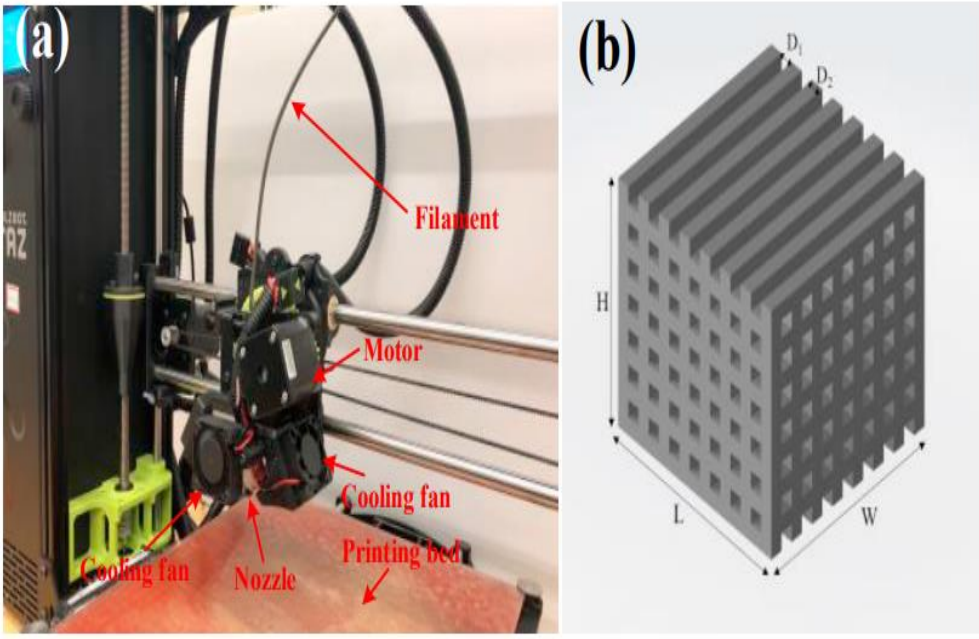

Fig. 5. (a) Lulzbot TAZ 6 3D printer (b) 3D structure of PLA-based scaffolds [10]

Table 1. FFF process parameters for fabrication of PLA-based scaffolds. [10]

Parameters	Value
Nozzle Temperature	205□
Bed Temperature	70□
Printing Speed	60 mm/s
Filament Diameter	2.85±0.15 mm
Layer Height	0.2mm
Infill Density	50%
Nozzle Size	0.5 mm

3.4 17–4 PH Steel:

A commercially available 17–4 PH Stainless Steel MIM raw material is directly utilized for 3D printing. Additional benefits include giving the printed item strength and making the polymers in composite feedstock simple to extract using thermal and solvent debinding processes. Following that, the parts' sintering could offer the density, shrinkage, and Moreover, the polyMIM feedstock's binders are simple to remove using solvent and thermal debinding processes, giving the printed item robustness. The additive manufacturing process flow of 17-4 PH steel is shown in fig.6. Subsequently, the parts' sintering might give them the density, shrinkage, and other characteristics that the MIM process gave samples. The Underlying feedstock for 3DEP's weakness, meanwhile, is its inability to maintain homogeneity while printing. [11]

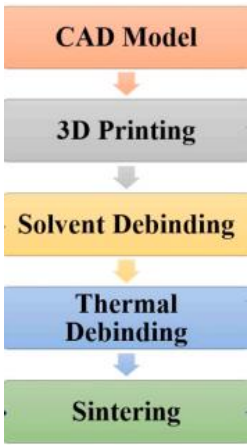

Fig. 6. Additive manufacturing process flow of 17–4 PH steel. [11]

3.5 Polymer–Nickel Composite:

The three polymers used in the work are —Polylactic Acid (PLA), Acrylonitrile Butadiene Styrene (ABS) and Poly Vinyl Butyral (PVB). Nickel powder of 99.7% purity is used as filler in the composite. The employed nickel powder particles ranged in diameter from 2.2 to 2.6 m, however they frequently aggregate to form larger, "chain-like" structures. Without additional purification, all of the reagents were employed in their original form. Moreover, nickel foam with a 0.5 mm thickness, 250 g/m2 surface density and of 100 ppi pore packing density is utilised as a support for the 3D printed parts. The element's mechanical strength is greatly increased by this support. For PLA based composite, melt mixing method is used and for PVB and ABS, solvent assisted method is used [18].

• **PLA-Ni Composite**

The polymer granules are weighed and then melted in a ceramic mortar at a temperature of 200□ on a heating plate. Nickel powder is added after it completely melted. To achieve nickel volume fractions of 5%, 10%, and 20% in the finished composite material, the polymer to nickel weight ratio is adjusted (see Table 4). A spatula was used to fully combine the mixture until it had a homogenous texture. The mixture is then evenly distributed on a foil base and left to harden. The detailed information of Substrates amount used for composite preparation; all samples prepared with 100 g of nickel powder is shown in Table. 2. The composite is removed after sometime and chopped into roughly 5mm X 5mm granules that could be used in the filament extrusion procedure. [18]

Table 2. Substrates amount used for composite preparation; all samples prepared with 100 g of nickel powder.

Polymer Used	Ni Volume Fraction in a Composite (vol%)	Polymer Amount (g)
PLA	5	264.7
	10	125.4
	20	55.7
PVB	10	111.31
	15	70.04
	20	49.58
	25	37.09

	50	12.37
ABS	10 20 25	105.19 46.82 35.03

• ABS-Ni and PVB-Ni Composites

ABS or PVB grains are weighed and then acetone is added as a solvent since they are soluble in acetone. A mixer is used to thoroughly agitate the mixture and dissolve the polymer. The mixing parameters are 800 rpm and a vacuum pressure of 90kPa for 10 minutes. Nickel powder is then added to the mixture in a precise amount. The mixture is reworked till it had a uniformly smooth consistency. The slurries are then applied evenly after pouring on the foil. They are then left for 2–3 days to completely vaporize the solvent. Then the composites were removed from the foil and grinded into fine granules. In this way, multiple composite materials with two distinct polymer matrices (ABS and PVB) and varying amounts of nickel powder were created. The Composite filament extrusion temperatures and speeds for selected composite materials, heating zones are numbered from screw to nozzle is shown in Table 3. The filler amounts used were 10%, 15%, 20%, 25%, and 50% by volume for each respective composite. Prior to extrusion, the granules produced using this method are properly dried and kept dry with the help of a desiccant. The Fabrication route of new composite filaments is shown in fig. 7. [18]

Table 3. Composite filament extrusion temperatures and speeds for selected composite materials; heating zones are numbered from screw (1) to nozzle (4). [18]

`	**PLA-Ni 5%**	**PVB-Ni 25%**	**ABS-Ni 25%**
Heaters		Set temperature(□)	
4	170	170	220
3	185	195	230
2	190	200	230
1	180	200	240
		Average extrusion speed(rpm)	
	~4.0	~3.0	~3.5

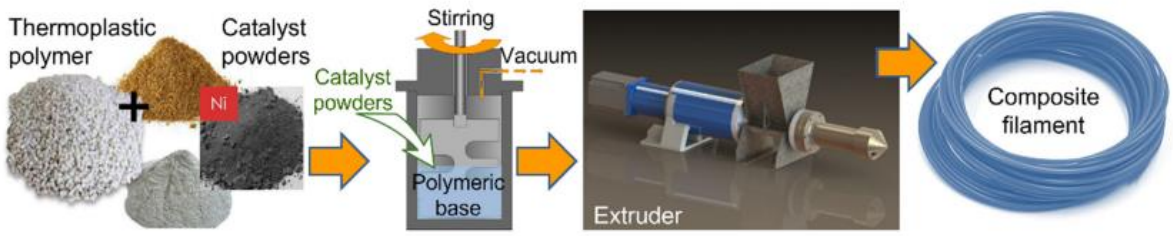

Fig 7. Fabrication route of new composite filaments. [18]

3.6 Copper-PLA:

A commercially available printer is used in the work [19]. and the print speed ranged from 50 to 150 mm/s. The filament is of diameter 1.75mm. Regular PLA (1.75 mm, white, 1.24 g/cm3) and ABS (1.75 mm, transparent, 1.05 g/cm3). and PLA with copper additive (PLA-Cu) (1.75 mm, 3.9 g/cm3) are chosen for the analysis. The slicing software Cura is used for all feedstocks to create the gcode files needed to print a puck with a diameter of 5.08 cm and a thickness of 0.52 cm (volume 10.5 cm3) with 20% in-fill. All materials are printed using the same g-code file, with the bed and print head temperatures adjusted as necessary. The Fused Filament Fabrication (FFF) printer and the enclosure chamber set up and materials is shown in fig. 8. The manufacturer's suggested temperature is 240. ABS extrusion attempts at 290 °C did not result in successful printing. [19]

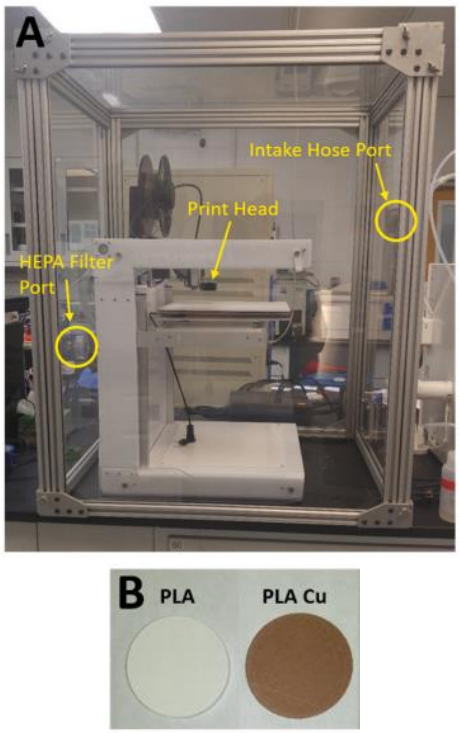

Fig. 8. A) Fused Filament Fabrication (FFF) printer and the enclosure chamber set up B) Materials

4. PRINTING

4.1 Ti-6Al-4V:

For both powder filament technologies, the feedrate's effect on the printing process is experimentally assessed. Four samples (10105 mm3) are taken at each feed rate. (using a MatterHackers Pulse 3D printer) are printed, and with a 3 g/cm3 filament density. The printed pieces with 100% density are projected to have mass about 1.5 grams. The fine powder filaments demonstrated good results in printing below a feed rate of 2 mm/s. Wide gaps in the structure were created by the non-uniform material deposition caused by an increase in feed rate above 4mm/s to 8mm/s. No printing occurred at all when the feed rate was increased further to 10 mm/s and above. The variation was 1.7 0.3% at 2 mm/s. When the feed rate was increased to 4 mm/s, the divergence was 6.8 0.9%. Feedrates above 8mm/s resulted in uneven material deposition resulting in defects in printed parts. Printing came to halt at feedrates above 14mm/s. As the feed rate increased, the dimensional discrepancy between the printed part and the CAD file followed a pattern resembling that of fine powder filaments. The deviation started off at 2.5 0.4% at 2 mm/s and decreased as feed rates increased, peaking at 5.5 1.3% at 6 mm/s. [6]

The printing range can be found out by comparing the force required to overcome the pressure drop of nozzle and the force that filament can withstand before failing. For Ti-6Al-4V filaments, increasing feed rate from 0.5 mm/s to 16 mm/s resulted in a increase of the force needed to overcome the pressure drop from 0.5 N to 2.35 N for fine powder filaments and from 0.25 N to 1.4 N for coarse powder filaments. It is discovered that the Ti-6Al-4V filaments, both fine and coarse ones, can withstand a force of 1N. The Effect of feed rate on the printed geometry is shown in fig. 9. MF3 printing would be successful if the force needed to overcome the pressure drop is kept below the filament's strength [6].

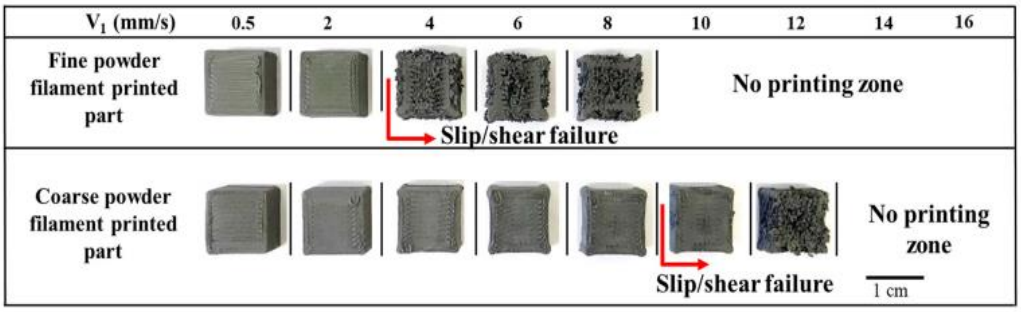

Fig. 9. Effect of feed rate on the printed geometry [6]

4.2 316L Stainless Steel:

To account for heavily loaded filaments' high viscosity and thermal material characteristics including their glass transition temperature (Tg) and melting point (Tm) are altered while printing with FFF technology. It takes temperatures greater than the melting point to sufficiently lower the filament's viscosity in nozzle to allow for extrusion. Adhesion will be improved if the bed temperature is a bit higher than the room temperature. Tg was lower than room temperature for the filaments that were exhibited. However, 100□ bed temperature is used to improve bonding of initial layer and to stop warpage. Polypropylene film served as the printing medium. For printing efficiency, a box geometry with a 5 mm wall thickness and an exterior length of 25 mm was used. In order to assess the printing quality, nozzle temperatures higher than 250 °C are chosen because the melting temperature of the filament being used is close to 220 °C. Initial printing tests revealed that for consistently reproducible printing of the material employed, 290□ was ideal. The densely loaded filament's viscosity is found to be too high for smooth extrusion at lower nozzle temperatures (below 270 °C). Increased nozzle temperatures (beginning at 295 °C) prevented freshly deposited strains from adhering well to lower layers, which prevented successful printing. The Fan speed – full, nozzle temperature-270 °C, Fan speed - optimal; nozzle temperature-290 °C and Fan speed-0; nozzle temperature 295 °C is shown in fig 10.

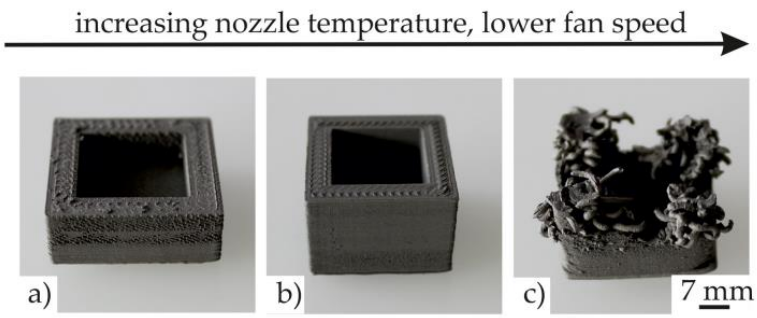

Fig. 10 (a) Fan speed – full; nozzle temperature-270 °C (b) Fan speed - optimal; nozzle temperature-290 °C (c) Fan speed-0; nozzle temperature 295 °C. [9]

4.3 PLA and 316L:

Compared to pure PLA, PLA-316L prints exhibited higher accuracy and reduced roughness of surface. Throughout the printing process, there are a number of significant elements that could have an impact on the pore size and strut width. According to the findings, adding 316L powders dramatically alters the characteristics of pure PLA. Loading capacity is clearly affected by the pore size. The range of 300 to 900 m is a reasonable range for average pore size, and also it is preferable to create the pore with a lower deviation. Consistent tissue growth might be made possible by homogenous distribution of holes, which could also avoid blockage in few areas of the prints and speed up the healing. The Surface morphologies of PLA-5 filament, PLA-5 scaffold, PLA-10 scaffold – voids observed and PLA15 scaffold - voids and gaps observation is shown in fig. 11. According to the literature, a rougher surface can aid in adherence and growth since a higher fluctuation could create more room for spreading of tissue and remodelling, which would improve the scaffolds' cytocompatibility [10].

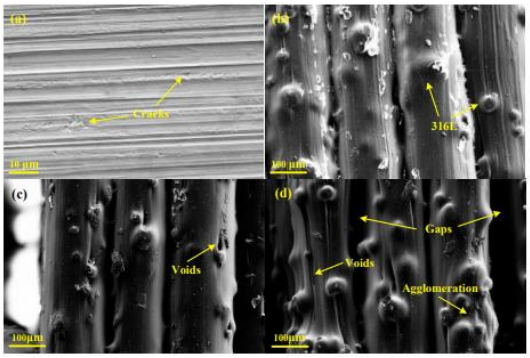

Fig. 11. Surface morphologies of (a) PLA-5 filament (b) PLA-5 scaffold; (c) PLA-10 scaffold – voids observed and (d) PLA15 scaffold - voids and gaps observed. [10]

4.4 17–4 PH Steel:

SolidWorks software was used to model the part through CAD (computer-aided design) and create a tessellated file. the tessellated file was sliced using the Simplify 3D programme. The sliced component is stored as a G-Code file. The screw-extruder for thermos mechanically deformable materials is what made the arrangement special. The screw extruder, which is situated in the infeed zone of vertically mounted extruder, has a substantially reduced length-to-diameter ratio and precludes rotational passage of material in funnel. For smooth feed to screw extruder, a pneumatically controlled piston, or "faker," was used. To ensure smooth printing, heaters were employed to modify the extrusion temperature. A typical FFF nozzle made up of hardened steel with 0.4 mm diameter, 13 mm in length, and 3 mm intake diameter is used to extrude the material. The binders in the MIM raw material provide the hot extrusion, as previously described, the necessary flowability. The Schematic diagram and picture of 3D printing machine used is shown in fig. 12. One thermal cycle is used to complete the sintering and thermal debinding processes in a tube furnace: 1□/min heating rate up to a thermal debinding temperature of (500□), soaking time of 1 hour, 4 C/C heating rate with 5 hours of soaking time, and 4 C/C cooling rate to 20□ in a He-4% and H2 atmosphere. Sintering temperatures of 1100 °C, 1200 °C, 1300 °C, and 1360 °C are selected [11].

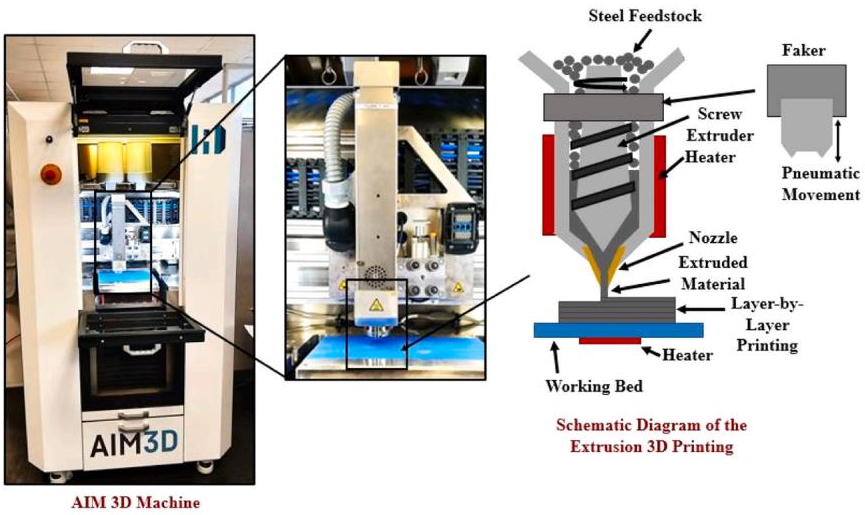

Fig. 12. Schematic diagram and picture of 3D printing machine used [11]

4.6 Polymer–Nickel Composite:

The printing materials for the FDM process were the polymer-Ni composite filaments created for these research. The Ultimaker S5 printer was used to prepare the parts. The study made use of a module for printing metallic filaments. A heating system is installed on the printing platform. A 3D part is created in the format compatible with the printer before printing. The printing programme was opened using the file that was retrieved. Two methods of 3D printing were used: one with and one without a nickel foam support. The composite material has been carefully matched to the printing parameters shown in Table 3. Printing was only done with composite filaments that were appropriate for this technique.

4.7 Copper-PLA:

The information reported here supports earlier research on clean ABS and PLA, showing ultrafine particles emissions during operation of 3D Printer. It is further shown that, even at constant temperature, doping common feedstocks with metal additions resulted in higher emissions for those materials. When this work is compared to other studies, it became clear how important it is to develop standardised testing procedures for ultrafine particles in order to fully comprehend and analyse the risks associated with 3D printers.. [19]

5. POST PROCESSING

5.1 Ti-6Al-4V:

It is observed from the fine powder filaments demonstrated good printability up to a feed rate of 2 mm/s. Wide gaps in the structure are created by the non-uniform material deposition caused by an increase of feed rate above 4mm/s to 8 mm/s. No printing occurred at all when the feed rate iss increased above 10 mm/s. The variation is 1.7±0.3% at 2 mm/s. When the feed rate was increased to 4 mm/s, the divergence was 6.8±0.9%. The stepper motor-determined travel movements seem to have some influence on the dimensional alterations. The use of servo motors has been recommended to produce improvement. [6]

5.2 316L Stainless Steel

After the completion of debinding, the final stage is sintering which would densify the parts. To prevent oxidation on the particle, all sintering experiments were conducted in a vacuum furnace surface. However, this does not eliminate any remaining C in the sample that is not destroyed by thermal debinding process. In order to save time, a heating rate of 0.3 °C/min was used during the thermal debinding process to evaluate the impact of sintering temperatures. The maximum

densifications are similarly observed at temperatures ranging 1300□ and 1360°C with dwell periods ranging from 60min and 240 min in sintering assessments of identical 316 L MIM components. The reported MIM part densities exceeded 98% of the anticipated density. However, after optimization of parameters throughout the SDS process, densities greater than 95% is repeatedly reached, even though the densities of the test series obtained for parts that are not manufactured at optimized parameters during all process steps. Since the fill grade is relatively lower for filaments (55vol%) when compared to MIM feedstocks (65vol%), the printed parts densities are lower than MIM parts [9].

5.3 PLA - 316L:

PLA-316L composite parts produced high dimensional accuracy depending on mean strut width, and mean pore size, and the inclusion of 316L powder further reduced surface roughness. When the steel powder filling is at 15 vol%, the surface roughness is found to be very low. In the immersion test for a month, swelling and layer delamination are seen in PLA and PLA-316L scaffolds, but no appreciable changes are found in impacts of 316L powder on degradation behaviour of the PLA-316L parts [10].

5.4 17–4 PH Steel:

The 3DEP green body's water-soluble polymer, PEG, was eliminated during the solvent debinding process. The samples were immersed in water for varying lengths of time and temperatures. The effect of immersion time on weight loss (%) at various temperatures. The specimens are sintered at various temperatures; 1100□, 1200□, 1300□, and 1360□, following thermal debinding. The relative density rises together with the sintering temperature. The sample sintered at 1360 C. had the maximum relative density, which was measured at 96.5%. displays the samples' microstructures. The microstructure readily reveals the geometrical variations in porosity with temperature. [11]

5.6 Polymer–Nickel Composite:

Organic moieties must be removed from the composite printed pieces after printing and before sintering using a technique that has been refined in earlier investigations. In a nutshell, the samples were sandwiched between two 1.6 mm thick ceramic (alumina) setters. The furnace was heated to a temperature of 200□ to begin heat treatment. The rate of heating was 5□/min. After heating the furnace up to 200□, a temperature step of two hours was utilised to eliminate volatile chemicals. The procedure was done in an air-filled environment. After that, the oven is heated to 400°C at a heating rate of 1°C/min. A reducing environment (95 percent N2 and 5 percent H2) was used for the heating procedure. To extract the polymeric binders, the conditions were maintained for two hours. The oven is finally heated to 800□ at a rate of 1□/min. Again, a reducing environment was utilised, and a temperature step of one hour is applied. This process is designed to thoroughly sinter the metallic particles, producing a porous substance. To stop nickel from oxidising during thermal treatment process, a reducing environment is used. the creation of open porous materials through 3D printing and into the finished product. [18]

Results and Discussions

It is important to understand the variation of different properties with respect to variation of different process parameters. Only then, we can choose the optimal conditions for printing an object successfully for respective application. In general, as already briefed, the main steps in this technique are; filament preparation, printing, and post-processing.

There are several parameters which need to be defined in each of the stages. For example, when we are making the filament from a single screw extruder, we need to define optimal temperatures of all the four heaters to obtain a filament of uniform diameter, free of defects and homogeneous composition [22]. Coming to printing, there are several process parameters such as build orientation, infill percentage, layer thickness, layer height, federate etc… which will affect one or the other mechanical properties. Literature has also shown that the post-

processing steps such as debinding and sintering can also alter the mechanical behaviour of final part. A few other variables are powder particle size, weight percentage of metal filler, heating rate in sintering etc…

To start with, Ti-6Al-4V based composites, which are made up of fine powdered particles showed different properties compared to that of coarse powdered particles. The extrusion of filament was successful at 105□ for both coarse and fine powdered filaments. But for coarser one, the density of filament was 99.8 ± 2%, whereas for finer one it was 3-4% higher [8]. In the work [6], the fine powdered composite was printed successfully at the federate of 2mm/s with a deviation of 1.7 ± 0.3%. Whereas, for coarse powdered composite, the optimal federate was 2mm/s – 6mm/s with a part deviation of 5.5 ± 1.3%. The solvent debinding process has been performed for Ti-6Al-4V – ABS composite since ABS is soluble in acetone. Here, when the wall thickness is greater than 4mm, it took more than 24 hours for successful debinding and for wall thickness less than 4mm, it was less than 24 hours [7].

Table.4. Variation of printability with variation of printing parameters and particle size

S.No	Particle size	Feedrate	Result	Part deviation
1	Fine	< 2mm/s	Success	1.7 ± 0.3%.
2	Fine	> 2mm/s	Fail	-
3	Coarse	< 2mm/s	Fail	-
4	Coarse	2mm/s - 6mm/s	Success	5.5 ± 1.3%
5	Coarse	> 6mm/s	Fail	-

According to literature [9], when 316L Stainless steel is mixed in 55% vol inn Polyolefin, the thermal debinding process has been performed unlike ABS. Here, it took 90 minutes and 750□ for complete debinding of backbone polymer. After which, the optimal sintering temperature was determined to be 1360□ and performed for a duration of 120 minutes. The final obtained part showed higher density and eliminated most of the pores formed while debinding with a linear isotropic shrinkage of 20%. Work is done on a similar composite in which the variation of mechanical properties with infill levels and build orientation were tested [25]. Fortunately, infill levels did not affect the final shrinkage percentage.

One more similar and popular composite was 17-4 PH Steel based filament which showed the higher tensile strength of 939.5 MPa when sintered at 1360□ for 3 hours with a shrinkage of 14.1%. The density was found to be 96.5%. Variation of hardness with sintering temperatures has also been observed, however, no considerable change in hardness is observed after 1200□ [11].

Table.5. Effect of Sintering duration on UTS

S.No	Filler	Sintering temperature	Sintering duration	Ultimate Tensile strength	Shrinkage
1	316 SS Steel	1360□	120 minutes	465 MPa	20%
2	17-4 PH Steel	1360□	180 minutes	939.5 MPa	14.1%

It has been also found that not all compositions are suitable for filament extrusion or printing. The outcomes of all the prepared composites and their suitability for filament extrusion are shown in table 6. For example, in the work [18], the better combinations of Polymer and Nickel are found to be PLA-Ni5%, PVB-Ni25%, and ABS-Ni25% (% in vol).

Table 6. Prepared composites and their corresponding filaments. [18]

Ni Powder vol% in Composite	PLA-Ni	PVB-Ni	ABS-Ni
50%	-	Unsuitable for extrusion (89 wt% of Ni)	-
25%	-	+ (73 wt% of Ni)	+ (74 wt% of Ni)
20%	Unsuitable for extrusion (64 wt% of Ni)	+ (67wt% of Ni)	+ (68 wt% of Ni)
15%	-	+ (59 wt% of Ni)	-
10%	Filament too brittle, it breaks (47 wt% of Ni)	+ (47 wt% of Ni)	+ (49 wt% of Ni)
5%	+ (27 wt% of Ni)	-	-

For popular emerging combinations like Cu-ABS [21], Al-ABS [22], attempts have been made to determine the optimum extrusion temperatures for filament fabrication and feedrate for printing.

It is already briefed that print orientation will also affect the final part's mechanical properties. Surprisingly, some orientations are not even possible for few combinations of metal and polymer [12,17]. The printability of the filament is equally important. The obtained green part should be free of defects, otherwise poor interlayers bonding occurs after sintering. Mechanical properties of parts that are obtained through Metal Fused Filament Fabrication were better than the thermoplastic parts which are metallized by electroplating [16,20]. MFFF parts showed similar mechanical properties to Metal Injection Moulding parts, but they are slightly poor when compared to the parts manufactured by standard Metal AM processes [17]. However, for the purpose of fabricating a low-cost prototype, this method is the best, since it consumes less energy hence making the process eco-friendlier.

Conclusion

- Metal Fused Filament Fabrication will stand out to be a cutting-edge technology owing to its lower energy consumption and sustainability. The entire process consists of four major steps; Filament preparation, Printing, Debinding, and Sintering.
- There are factors which play a key role in each of the steps. During the stage of filament preparation; particle size, particle shape, percentage of filler, mixing method, extrusion method, and extrusion temperatures affect the final homogeneity of the filament. Meanwhile, printing parameters such as infill percentage, feedrate, layer height, layer thickness, cooling rate, part orientation will play a major role.

- The debinding method to be performed will depend on the polymer used. And Sintering temperatures will depend on metal, polymer, and their composition also.
- The optimum conditions for any of the stages of MFFF process have not been determined yet for any single composite. This opens a great scope for future research to develop advanced technologies and materials which can be used in this process.
- MFFF will enable further opportunities in the fields of aerospace, automotive, medicine, education etc…

Future Scope

MFFF technology will give an opportunity for future research in the following areas;

1. Development of new composites of novel materials ranging from conductive metals to nano materials.
2. The development of simulation tools for predicting the suitability of composition for filament extrusion.
3. The development of new algorithms for predicting the suitable extrusion temperatures and screw speed for filament extrusion.
4. The development of new simulation tools which can show the printing process virtually based on the defined parameters.
5. The innovation of enhanced simulation tools that, when given inputs like as material properties, processing parameters, and construction techniques, can forecast the characteristics of constructed parts.
6. The improvement of screw-based AM machines to take raw material in the form of pellets to eliminate the complexity of filament fabrication which in turn enables higher percentage of metal fillers that can be added into polymer.
7. Innovation of new simulation tools which can predict the optimum debinding temperature and duration for thermal debinding process based on the composition of metal and polymer.
8. Innovation of new simulation tools which can predict the optimum duration and solvent for solvent debinding process based on polymer and its weight or volume percentage.
9. The scope to develop new software which can integrate all the four processes of MFFF in a single solution.

References

1. Ngo, T. D., Kashani, A., Imbalzano, G., Nguyen, K. T., & Hui, D. (2018). Additive manufacturing (3D printing): A review of materials, methods, applications and challenges. Composites Part B: Engineering, 143, 172-196.
2. Shahrubudin, N., Lee, T. C., & Ramlan, R. J. P. M. (2019). An overview on 3D printing technology: Technological, materials, and applications. Procedia Manufacturing, 35, 1286-1296.
3. Park, S., & Fu, K. K. (2021). Polymer-based filament feedstock for additive manufacturing. Composites Science and Technology, 213, 108876.

4. Roshchupkin, S., Kolesov, A., Tarakhovskiy, A., & Tishchenko, I. (2021). A brief review of main ideas of metal fused filament fabrication. Materials Today: Proceedings, 38, 2063-2067.
5. Angelopoulos, P. M., Samouhos, M., & Taxiarchou, M. (2021). Functional fillers in composite filaments for fused filament fabrication; a review. Materials Today: Proceedings, 37, 4031-4043.
6. Singh, P., Balla, V. K., Tofangchi, A., Atre, S. V., & Kate, K. H. (2020). Printability studies of Ti-6Al-4V by metal fused filament fabrication (MF3). International Journal of Refractory Metals and Hard Materials, 91, 105249.
7. Zhang, Y., Bai, S., Riede, M., Garratt, E., & Roch, A. (2020). A comprehensive study on fused filament fabrication of Ti-6Al-4V structures. Additive Manufacturing, 34, 101256.
8. Singh, P., Balla, V. K., Atre, S. V., German, R. M., & Kate, K. H. (2021). Factors affecting properties of Ti-6Al-4V alloy additive manufactured by metal fused filament fabrication. Powder Technology, 386, 9-19.
9. Thompson, Y., Gonzalez-Gutierrez, J., Kukla, C., & Felfer, P. (2019). Fused filament fabrication, debinding and sintering as a low cost additive manufacturing method of 316L stainless steel. Additive Manufacturing, 30, 100861.
10. Jiang, D., & Ning, F. (2020). Fused filament fabrication of biodegradable PLA/316L composite scaffolds: Effects of metal particle content. Procedia Manufacturing, 48, 755-762.
11. Singh, G., Missiaen, J. M., Bouvard, D., & Chaix, J. M. (2021). Additive manufacturing of 17–4 PH steel using metal injection molding feedstock: Analysis of 3D extrusion printing, debinding and sintering. Additive Manufacturing, 47, 102287.
12. Patel, A., & Taufik, M. (2021). Nanocomposite materials for fused filament fabrication. Materials Today: Proceedings, 47, 5142-5150.
13. Sargini, M. I. M., Masood, S. H., Palanisamy, S., Jayamani, E., & Kapoor, A. (2021). Additive manufacturing of an automotive brake pedal by metal fused deposition modelling. Materials Today: Proceedings, 45, 4601-4605.
14. Liu, Z., Lei, Q., & Xing, S. (2019). Mechanical characteristics of wood, ceramic, metal and carbon fiber-based PLA composites fabricated by FDM. Journal of Materials Research and Technology, 8(5), 3741-3751.
15. Gonzalez-Gutierrez, J., Cano, S., Schuschnigg, S., Kukla, C., Sapkota, J., & Holzer, C. (2018). Additive manufacturing of metallic and ceramic components by the material extrusion of highly-filled polymers: A review and future perspectives. Materials, 11(5), 840.
16. Romani, A., Mantelli, A., Tralli, P., Turri, S., Levi, M., & Suriano, R. (2021). Metallization of thermoplastic polymers and composites 3D printed by fused filament fabrication. Technologies, 9(3), 49.
17. Tosto, C., Tirillò, J., Sarasini, F., & Cicala, G. (2021). Hybrid metal/polymer filaments for fused filament fabrication (FFF) to print metal parts. Applied Sciences, 11(4), 1444.

18. Mackiewicz, E., Wejrzanowski, T., Adamczyk-Cieślak, B., & Oliver, G. J. (2022). Polymer–Nickel Composite Filaments for 3D Printing of Open Porous Materials. Materials, 15(4), 1360.
19. Alberts, E., Ballentine, M., Barnes, E., & Kennedy, A. (2021). Impact of metal additives on particle emission profiles from a fused filament fabrication 3D printer. Atmospheric Environment, 244, 117956.
20. Zhan, J., Tamura, T., Li, X., Ma, Z., Sone, M., Yoshino, M., ... & Sato, H. (2020). Metal-plastic hybrid 3D printing using catalyst-loaded filament and electroless plating. Additive Manufacturing, 36, 101556.
21. Sa'ude, N., Ibrahim, M., Ibrahim, M. H. I., Wahab, M. S., Haq, R., Marwah, O. M. F., & Khirotdin, R. K. (2018). Additive manufacturing of copper-ABS filament by fused deposition modeling (FDM). Journal of Mechanical Engineering (JMechE), (4), 23-32.
22. Kumar, N., Jain, P. K., Tandon, P., & Pandey, P. M. (2019). Investigations on the melt flow behaviour of aluminium filled ABS polymer composite for the extrusion-based additive manufacturing process. International Journal of Materials and Product Technology, 59(3), 194-211.
23. Mousapour, M., Salmi, M., Klemettinen, L., & Partanen, J. (2021). Feasibility study of producing multi-metal parts by Fused Filament Fabrication (FFF) technique. Journal of Manufacturing Processes, 67, 438-446.
24. Mousapour, M., Salmi, M., Klemettinen, L., & Partanen, J. (2021). Feasibility study of producing multi-metal parts by Fused Filament Fabrication (FFF) technique. Journal of Manufacturing Processes, 67, 438-446.
25. Ait-Mansour, I., Kretzschmar, N., Chekurov, S., Salmi, M., & Rech, J. (2020). Design-dependent shrinkage compensation modelling and mechanical property targeting of metal FFF. Progress in Additive Manufacturing, 5, 51-57